Received: 10 February 2022 | Revised: 12 June 2022 | Accepted: 30 June 2022

IET Generation, Transmission & Distribution

DOI: 10.1049/gtd2.12556

The Institution of Engineering and Technology WILEY

ORIGINAL RESEARCH

Adaptive control and management of multiple nano-grids in an islanded dc microgrid system

Seyyed Ali Ghorashi Khalil Abadi[1] | **Tohid Khalili**[1] | **Seyed Iman Habibi**[1] | **Ali Bidram**[1] | **Joseph M. Guerrero**[2]

[1]Department of Electrical & Computer Engineering, University of New Mexico, Albuquerque, New Mexico, USA

[2]Department of Energy Technology, Aalborg University, Aalborg, Denmark

Correspondence
Seyyed Ali Ghorashi Khalil Abadi, Department of Electrical & Computer Engineering, University of New Mexico, MSC01 1100, Albuquerque, NM, USA.
Email: ghorashi@unm.edu

Funding information
National Science Foundation EPSCoR Program under Award #OIA- 1757207

Abstract

This paper presents an adaptive control framework for the flexible and effective management and control of clustered DC nano-grids (NGs) in an islanded DC microgrid system. It is assumed that each NG contains a photovoltaic (PV) system, a battery energy storage system (BESS), local loads, and a gateway (GW) module. Each NG has a hierarchical control system consisting of a decision-making module and low-level controllers. The decision-making module ensures various desirable features including plug-and-play operation of NGs, maximum utilization of PV power generations, and avoiding state of charge (SoC) violation of batteries. Moreover, an adaptive model predictive control (AMPC) strategy is proposed to regulate the voltage of the NG local DC buses in the presence of non-linear loads. This approach improves the performance of the NG voltage control system and reduces the current ripples of BESSs, thereby enhancing the lifetime of the batteries. In addition, a smart switching consensus-based control strategy is designed that provides flexible power sharing among the NGs to balance the SoC of BESSs in which the BESSs altogether imitate the behaviour of a single cloud energy storage system (ESS). Finally, the performance of the proposed control system is verified by simulating the DC microgrid in MATLAB/Simulink.

1 | INTRODUCTION

Micro-grids (MGs) are independent active distributed energy systems that can improve the performance of traditional power systems through increasing consumer participation, sustainable energy resources penetration, grid resiliency, and power system stability [1]. Designing MGs by connecting multiple nano-grids (MNGs) promotes the modularity of MGs which in turn results in higher flexibility, resiliency, and scalability [2]. Nano-grids (NGs) can be defined as power distribution systems consisting of local power generation and consumption units which conventionally include a local energy storage system (ESS), a gateway (GW) module, and a dedicated control system [3]. NGs share lots of features with MGs such as operation in isolated or grid connected mode. However, they have smaller scale and simpler structure, typically, supplying a building or a single load [3, 4]. While NGs can be AC, more recently, DC NGs have gained much attention to minimize power conversion losses and reduce the system complexity [2]. MNGs have a different structure compared to conventional DC MGs requiring control and management strategies which are well suited for their structural features.

1.1 | Power management strategies in DC MNGs

In islanded DC MGs, typically, there are multiple distributed energy resources (DERs) which are connected in parallel to the MG common DC bus through power electronic converters and they are responsible for regulating the DC bus voltage as well as for maintaining the stability of the system (i.e. grid-forming units) [5]. The efficient and reliable operation of these parallel grid-forming units requires appropriate power sharing strategies that can be achieved using centralized, decentralized, or distributed control approaches. However, the conventional

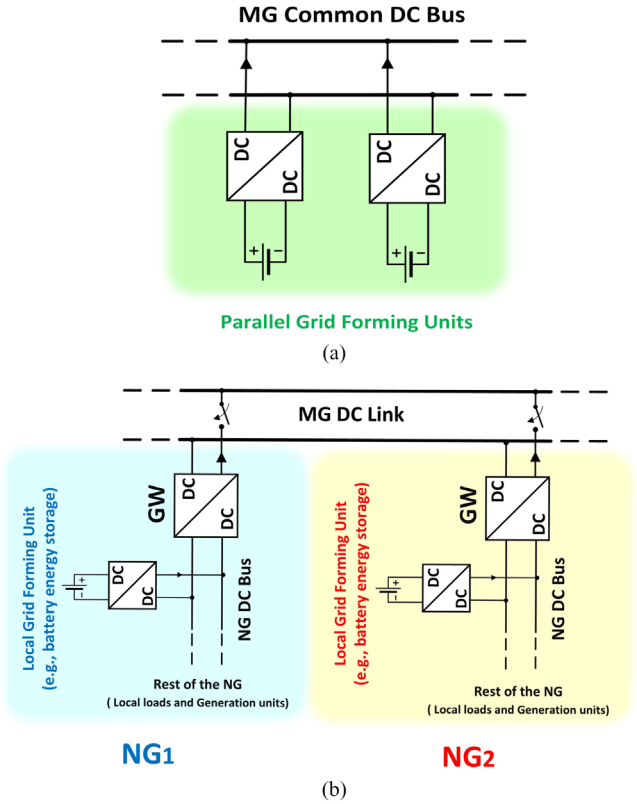

FIGURE 1 Structure of DC MGs: (a) a typical DC MG with parallel grid-forming units; (b) a DC MG that consists of multiple DC NGs (i.e. a DC MNG system). MG, micro-grids; NG, nano-grids.

control and power management techniques designed for parallel connected DERs may not be feasible in islanded MNGs due to their different structure. Figure 1 compares the structure of a typical islanded DC MG with an MNG system. As seen, in an MNG system, there is one grid-forming unit at each NG (e.g. a battery energy storage system [BEES]) that regulates the NG local DC bus voltage, and the GW module is responsible for power exchange with the upstream grid. In this structure, the local grid-forming units are connected to different DC buses to supply their local loads. Consequently, in an MNG, local grid-forming units cannot directly coordinate, and the effective power sharing of MNG requires an advanced coordination among the GW modules of different NGs. On the other hand, the plug and play (PnP) operation of NGs is a vital requirement for reliable and scalable operation of an MNG system. Therefore, the effective operation of clustered NGs requires a highly flexible and adaptive control and management system to provide a desirable power sharing among different NGs without affecting their PnP ability [6–8].

To address the discussed challenges, a variety of centralized, decentralized, and distributed control schemes have been suggested in the literature for MNG systems. In centralized control architectures, typically one NG or a cloud energy storage (e.g. the community BESS) operates as a master unit to control the voltage of the MG common DC bus using its GW converter (i.e. the MG grid-forming unit) and the other NGs operate as grid following units and exchange power with each other through their GW modules [9]. Despite simplicity, this approach may put considerable stress on the master unit when the number of NGs is high, and/or the NGs. Power generation and load fluctuate a lot. Reference [10] proposes a modified centralized control scheme for multiple NGs in an AC MG. The proposed system contains a photovoltaic (PV)/ BESS as a master unit and three other NGs. In this approach, to reduce the burden on the master unit, the grid following NGs demands constant active power. However, if the active power demand inside each NG varies significantly over time, the accurate power sharing among the NGs cannot be provided.

Alternatively, the decentralized and distributed control structures can be deployed to increase the flexibility and scalability of the control system. Reference [11] proposes a decentralized control strategy in an islanded cluster of NGs to provide flexible power sharing and voltage regulation inside the system. In this method, power exchange among the NGs is based on the variation of the common DC bus voltage, and the participation of BESSs in voltage regulation of local DC buses is related to their available capacity or state of charge (SoC). A decentralized power sharing strategy between DC NGs based on a non-linear I–V droop control technique is also proposed in [12]. This method improves the power sharing in the DC MNG systems and provides less steady-state voltage deviation compared to the conventional power-sharing methods with linear droop characteristic. Reference [13] also proposes a distributed voltage control and power-sharing strategy in an MNG system using a consensus control protocol. The ability of the proposed control algorithm in realizing the global power objective and voltage profile, while mitigating different types of attacks has been studied. However, neither [11] nor [13] has addressed the battery SoC balancing performance in different NG units.

Effective SoC balancing is of paramount value in MGs with multiple ESSs to increase their efficiency and MG's reliability [14]. The SoC balancing control strategies in DC microgrids with parallel distributed ESSs have been widely discussed in the literature [15–17]. In these methods, the contribution of an ESS to voltage regulation of the MG DC bus is conventionally related to its available capacity or SoC. However, as discussed before, the ESSs are connected to different DC links (i.e. each ESS is responsible for voltage regulation of its local DC bus) in MNG systems and the direct coordination among the ESSs is not available. In addition, the local loads and generation units in different NGs may have considerably different power profiles. This can provide situations in which a BESS in one NG is charging while a BESS in another NG is discharging. Moreover, the NGs should be able to safely disconnect and connect to the MG DC bus at any time (i.e. PnP operation) [7]. When an NG is connected to MG common DC bus, it can share power with other NGs through its GW module to balance the SoC of its BESS with them. But, if the NG is isolated, it may still continue to supply its local loads without the ability of power exchange with its neighbouring NGs. So, the battery SoC balancing strategies in MNGs should be highly adaptable to the operational modes of the NGs to ensure the PnP operation of them. In conclusion, due to the different structure of MNGs,

the conventional power-sharing methods designed for parallel BESSs in conventional DC MGs are not feasible for battery SoC balancing in MNG systems [18, 19]. To address this issue, an additional control layer (e.g. a supervisory control system) is suggested to improve the flexibility of the system by adjusting the control setting of the NGs based on the system conditions [18]. For instance, a decentralized adaptive droop control strategy is proposed in [18] which provides a communication-less coordination among NGs to balance the SoC of BESSs. The NGs contain a PV, household loads, and a BESS that regulates the NG local DC bus voltage. In this method, there is a supervisory controller that selects the operational mode of the NGs with respect to the SoC of their local BESS and common DC bus voltage. Despite the high level of scalability and flexibility, this approach has the following drawbacks: The proposed I–V droop control approach may cause relatively high voltage deviation on the MG DC link (i.e. %5) as well as inaccurate power sharing among NGs which are the intrinsic limitations of the decentralized droop control techniques [20, 21].

1.2 | Voltage regulation of local DC buses

In addition to the importance of incorporating a flexible battery SoC balancing and power-sharing strategy among NGs, designing an effective control technique for regulating NG's local DC bus voltage is of paramount value. Generally, there is one grid-forming unit at each NG (e.g. a BESS) that regulates the NG local DC bus voltage (i.e. the local grid-forming unit). The NG local DC bus voltage control system generally consists of two cascaded proportional-integral (PI) controllers and a pulse width modulator (PWM) which is similar to the conventional primary control layer of DC MGs. In this structure, the reference voltage for the PI voltage controller is typically a constant value (i.e. the nominal voltage of the NG DC bus). However, when a DC MG that consists of multiple NGs (i.e. an MNG system) is islanded, at least one of the NGs should regulate the MG common DC bus voltage through its GW module to maintain the stability of the islanded MG. In this case, the GW module is seen as a constant power load (CPL) or a constant power source (CPS) from its NG local DC bus point of view based on the direction of its output current. Consequently, the DC NGs intrinsically face with the CPL issue that cannot be effectively addressed with the conventional PI voltage regulators [22–24]. Due to the small size of NGs, this CPL issue does not usually destabilize the NG. But it may cause low marginal stability and some voltage oscillations on the NG local DC bus, especially if the DC NG contains some local CPLs [25]. These voltage oscillations can produce large current ripples of the local grid-forming DER. Knowing that the local grid-forming unit in DC NGs is typically a BESS, these current ripples can significantly reduce BESS lifetime [26, 27]. Therefore, a more advanced NG voltage control strategy is desirable to increase the system efficiency and reliability.

To tackle this challenge, model predictive controllers (MPC) can be utilized to regulate the NG's local DC bus voltage. MPC techniques are among the alternatives of PI controllers in systems with CPLs that can provide an optimal tradeoff between voltage variation, modification of load impedance, and the current ripples of energy storages [28–30]. Thus, implementation of an appropriate MPC algorithm can improve the transient response and dynamic stability of the NGs as well as increasing the life-time of the BESS compared to the regular PI controllers. The key idea of the MPC is to utilize a dynamical model of the system to predict its future response and apply it to compute a sequence of future control input actions. To this end, typically, the linearized model of the system around an operating point is utilized to predict the future responses [28]. Among many available MPC techniques, direct MPC with reference tracking which is also known as finite control set MPC (FCS-MPC) is the most popular method in the literature for DC power applications because of its intuitive design procedure and straightforward implementation [31, 32]. This approach does not incorporate any modulator (e.g. pulse width modulation [PWM] unit) and it aims to achieve the regulation of output variables (e.g. output voltage or current) along their reference trajectories by directly manipulating the converter switches. However, this method may lead to computationally interactable optimization problems due to its computational complexity [33]. Additionally, due to the removal of the PWM unit, the direct MPC method suffers from a variable switching frequency which complicates the design of converter's output filters [34]. Moreover, as illustrated in Figure 2, the required sampling time for the direct MPC approach is in the range of few microseconds which demands

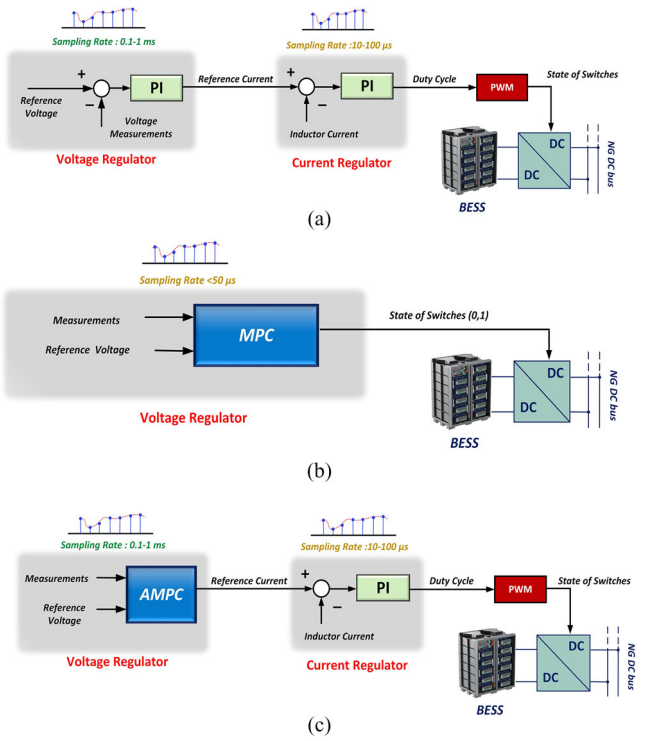

FIGURE 2 Control structure of the local grid-forming DER in DC MGs: (a) conventional PI control structure; (b) direct or FCS-MPC method; (c) the proposed AMPC-PI method. AMPC, adaptive model predictive control; DER, distributed energy resources; FCS, finite control set; MPC, model predictive controllers; PI, proportional-integral.

significantly more sophisticated hardware for real-time applications compared to the conventional PI voltage regulators. Consequently, the implementation of this technique requires a major restructuring of the local grid-forming control and measurement systems that may not be always viable. Furthermore, because the output power of the GW module varies significantly over time, the DC NG has a non-linear time-varying dynamic behaviour. Thus, the effective and reliable operation of the DC NG may not be ensured using linear control (e.g. PI controllers) or conventional MPC techniques. To tackle this issue and improve the performance of the NG voltage control system, adapting the NG voltage controller is needed with respect to the system changes [35].

1.3 | Contribution and scope

To address the discussed challenges, this paper proposes an adaptive and flexible distributed control framework for a cluster of NGs in an islanded DC microgrid. The contributions of this paper are threefold

1) To increase the flexibility of the MG voltage control and power management system, ensure the PnP operation of the NGs, maximize PV power generation, and avoid battery SoC violation, an advanced rule-based supervisory control system (a decision-making module) is designed for each DC NG. The supervisory controller adjusts the operational mode of the NG components (e.g. GW, BESS, PV, and load) with respect to system conditions (or based on some predefine rules) to achieve the system objectives. The discrete logic of the supervisory controller is designed using a unified modelling language (UML) state diagram. This framework has the ability to represent the nested states and concurrent operation of the NG components that significantly reduces the complexity of system design compared to conventional finite state machines with sequential Boolean logics. In another word, the proposed UML structure facilitates the design of more advanced logic for the NG management systems, thereby improving the flexibility and adaptability of the NGs in a distributed and scalable manner. As a result, the proposed NG management strategy supports a variety of features such as autonomous PnP operation of NGs, maximizing PV power generation and BESS SoC management.
2) An adaptive distributed power-sharing strategy is proposed based on a smart switching averaging consensus protocol to promote the system flexibility and efficiency by offering an accurate battery SoC balancing among different NGs while maintaining the PnP operation of NGs. In this method, the BESSs of all NGs that are not isolated maintain the same SoC value at their steady-state operation. Thereby, the BESSs imitate the behaviour of a single-cloud energy storage whose capacity is equal to the summation of all the BESSs' energy storage capacities. Moreover, this approach provides a significantly less voltage deviation on the MG's common DC bus compared to the decentralized adaptive droop control techniques. One of the main differences of the proposed smart switching consensus algorithm with other switching consensus techniques is that in this method the communication network is fixed but the signals that agents transfer via the communication network are changed based on predefined rules using a rule-based supervisory controller to track the changes on the electrical network and system objectives. Therefore, the communication network is less complex, but it is smart and more flexible. Table 1 clarifies the advantage of the proposed adaptive distributed SoC balancing method and compares it with the discussed power-sharing strategies in the DC MNG systems.
3) An adaptive model predictive control (AMPC) algorithm is utilized to regulate the voltage of the NGs' local DC bus in the presence of time varying and non-linear behaviour of the GW modules as well as the local CPLs. This method maintains the structure of the conventional NG voltage control system, but the PI voltage regulator is replaced by an AMPC controller. In this approach, the AMPC controller is cascaded with a PI current regulator, and indirectly regulates the NG local DC voltage by computing a reference trajectory for the current regulator. In addition, the required sampling time for the AMPC controller is in the range of a millisecond which is approximately similar to the sampling time of the conventional digital PI voltage regulators in DC NG applications. In addition, the design of converter output filter remains similar to the conventional cascaded PI controllers with PWM techniques. Consequently, the implementation of this technique does not require a noticeably more sophisticated hardware or a major restructuring of the conventional NG voltage control systems. Finally, the simulation results show that the proposed control strategy can reduce the stress on the BESS module compared to the regular PI voltage controllers as well as improving the transient response of the system. Figure 2 compares the structure of the proposed technique with the conventional PI and direct MPC methods, and Table 2 clarifies the advantage of the proposed technique compared to the existing methods discussed in the literature review.

The rest of this paper is organized as follows: Section 2 discusses the main control challenges in islanded DC MNGs, Section 3 describes the proposed system architecture. Section 4 discusses the designed supervisory controller (i.e. the internal logic of the agents). Section 5 first formulates an AMPC algorithm for regulating the voltage of the NGs' local DC buses, and then presents a distributed control strategy for power sharing (or battery SoC balancing) and regulating the voltage of the MG common DC bus. The proposed multiagent-based control strategy is verified through computer simulation in Section 6. Section 7 discusses the future research direction, and Section 8 concludes the paper.

2 | CONTROL CHALLENGES IN ISLANDED DC MNGS

This section discusses the specific control challenges in islanded DC MNGs including the GW behaviour as a CPL or a CPS in local DC buses as well as the flexible power-sharing

TABLE 1 Different power sharing and battery SoC balancing strategies in MNG systems

Structure	METHOD	Advantage	Disadvantage
Centralized	Centralized management for optimal operation [9].	Optimal/economical power sharing.	Low scalability, low reliability, high stress on the master unit.
	Modified centralized method with constant active power exchange [10].	Reduced stress on the master unit.	Inaccurate power/current sharing.
Decentralized	Self-sustained decentralized power exchange [12].	Reliable, communication-less, easily scalable.	Steady-state voltage deviation, inaccurate current sharing.
	Adaptive decentralized power sharing for battery SoC balancing [19].	PnP operation of NGs is provided, reliable, communication-less.	High steady-state voltage deviation.
	Decentralized non-linear I–V droop technique for power exchange in clustered DC NGs [13].	PnP operation of NGs, reliable, communication-less.	Degraded performance in large-scale systems.
Distributed	Secured consensus-based distributed control of clustered DC NGs [14].	Reliable, robust against cyber-attack, accurate current sharing.	PnP operation of NGs is not provided.
	This paper's proposed adaptive distributed power sharing and battery SoC balancing method.	Flexible to system changes, autonomous PnP operation of NGs, accurate current sharing, high-quality voltage.	Relatively complex decision logic.

TABLE 2 Characteristics of the conventional PI and MPC control techniques for the grid-forming unit of DC MGs

Strategy	Switching frequency	Sampling rate	Flexibility	CPL tolerance
Conventional cascaded PI	Fixed (simple filtering).	0.1–1 ms	Relatively flexible to system changes.	Poor transient response or instability.
Direct or FCS-MPC	Variable (complex filtering).	<50 μs	Prediction model cannot be updated (inflexible).	Accurate response for CPLs around nominal operating point. The performance can be affected if the CPLs significantly vary overtime.
Proposed AMPC-PI	Fixed (simple filtering).	0.1–1 ms	Prediction model is updated based on system changes (flexible).	Acceptable transient response for different CPL/CPS values.

challenges. The rest of this paper will focus on addressing these challenges.

2.1 | CPL and CPS behaviour of the GW in local DC buses

As illustrated in Figure 1b, there is a local grid-forming DER (e.g. a BESS) at each NG that is responsible for regulating the local DC bus voltage. In addition, the DC NGs can share/exchange power in the MNG network through their GW modules. In another word, the GW converters connect the local DC buses to MG common DC to support the power sharing between DERs of different NGs. Moreover, in islanded DC MNGs, at least one of the NGs should operate as the network grid-forming unit to regulate the MG common DC bus voltage through its GW module. Therefore, the GW units play two different roles at the same time. From the MG DC link point of view (see Figure 1b), they behave similar to a controlled voltage source to regulate the MG DC link voltage. On the other hand, from their local DC buses, they operate like a current source that demands or injects power regardless of the transient voltage variation at the NG local DC bus. Therefore, from the local

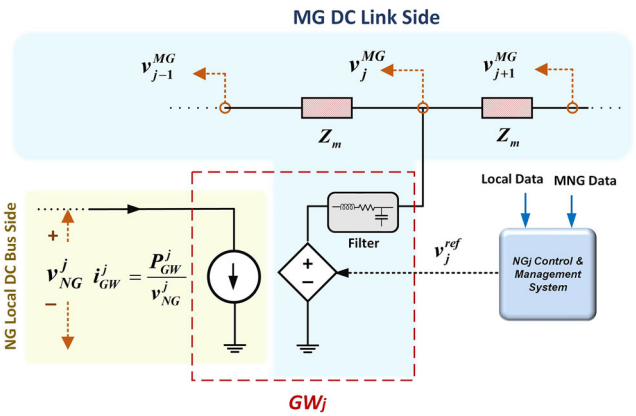

FIGURE 3 The simplified schematic model of grid-forming GWs in MG and NG DC buses. GW, gateway.

DC bus point of view, the GW module behaves as a CPL, or a CPS based on the direction of its output power. Figure 3 shows the schematic model of the GW from local and common DC buses point of view. Based on this model, and assuming the line inductance is negligible, the output power of the GW is obtained

as

$$P_{\mathrm{GW}}^{j} \simeq \frac{v_j^{\mathrm{MG}}(v_j^{\mathrm{MG}} - v_{j-1}^{\mathrm{MG}})}{R_m} + \frac{v_j^{\mathrm{MG}}(v_j^{\mathrm{MG}} - v_{j+1}^{\mathrm{MG}})}{R_m} \quad (1)$$

where v_j^{MG} represents the output voltage of the GW converter of NG_j and R_m is the line resistance. Also, v_{j-1}^{MG} and v_{j+1}^{MG} show the output voltage of the GW modules of the neighbouring NGs. Equation (1) clearly shows that the power transferred by GW from the NG local DC bus to the MG DC link is not related to the local DC bus voltage. This means that, from the local DC bus point of view, the GW module is seen as a CPL if $P_{\mathrm{GW}}^{j} > 0$ and it will be seen as a CPS if $P_{\mathrm{GW}}^{j} < 0$. It should be noted that the output power of the GW which also represents the amount of power exchanged among NGs is typically controlled by adjusting the reference voltage of the GW converters (i.e. v_j^{ref}) through the MNG energy management or power-sharing system (Note: at steady state $v_j^{\mathrm{ref}} \simeq v_j^{\mathrm{MG}}$).

The discussed behaviour of the GW modules may cause some major voltage stability issues in local DC buses that are explained as follows:

- In the case of CPL operation of GWs, they significantly reduce the marginal voltage stability of their local DC bus due to their negative incremental resistance, thereby impacting the functionality of conventional PI controllers. This means that voltage control techniques should be utilized that can effectively address the CPL issue.
- The GW modules cause a significant variation on the nominal operating point of DC NGs. For instance, they may operate as a CPS when they are transferring power to the local DC bus and a few hours later they may behave like a CPL when they are sending power to the MG DC link. Therefore, due to the fact that the CPL units and CPS units have opposite impacts on the dynamic behaviour of DC power systems, the voltage control techniques that utilize the linear approximation of the system' s model around a fixed nominal point (i.e. linear controllers or conventional MPC methods) will be dysfunctional. This means that voltage control techniques should be implemented which can adapt themselves to the ever-changing behaviour of the system.

2.2 | Flexible power sharing and PnP operation of NGs

As discussed in Section 1.1, due to the fact that the local BESSs of different NGs are connected to different DC buses, the conventional droop-based techniques cannot achieve desirable power sharing among BESSs to balance their SoC values (see the MNG structure in Figure 1). To effectively balance the SoC of BESSs additional information exchange among NGs such as SoC of BESSs and connection status of NGs are required. Typically, this coordination can be achieved using centralized control architectures in which all DC NGs inside the system communicate with the centralized supervisory control and energy management system (EMS). However, the centralized technologies cause low reliability, lack of scalability, and vulnerability to a single point of failure. The decentralized DC bus signalling methods can also provide a seam-less coordination between the NGs, but they generate a large voltage deviation on the MG common DC link (e.g. 2%–5%) [18]. On the other hand, the conventional averaging consensus algorithms with fixed network topology, which are widely used for distributed control techniques in DC MGs, are not suitable for SoC balancing of BESSs in DC MNGs because the available NGs for power sharing or the number of grid-forming GW units can be changed during the system operation. To address this issue, communication network topology of the system should be able to follow the system changes and switches to the new configurations according to the system conditions. Therefore, consensus-based algorithms with switching topologies are needed. Yet, changing the network topology is not the only issue in DC MNG systems. The power sharing and BESS SoC balancing can be more complicated in these systems if the PnP operation of NGs is an objective of the control system. The reason is that the distributed power sharing among NGs is realized by adjusting the reference voltage of the grid-forming GW modules based on the SoC value of BESSs. However, assume a case that an isolated DC NG immediately reconnects to the MG common DC link. If the BESS's SoC of that NG significantly differs from the other NGs who are currently connected to the MG DC link, which is highly probable, the distributed power-sharing algorithms may compute a large voltage deviation that can destabilize the system or activate the protection relays. Therefore, an additional intelligent control layer (i.e. a real-time decision-making module) at each NG is required to not only change the operating mode of the NG components but also adjust the switching consensus algorithm based on the sequence of previous actions of the NG components and neighbouring agents as well as the current system conditions. In another word, to guarantee the smooth PnP operation of NGs, the distributed consensus algorithm and NG management system needs some intelligence with high-level adaption. On the other hand, due to the concurrent behaviour of NG components, designing the required advanced logic of the decision-making system by standard techniques such as FSMs or state flow charts can be a tedious task. Therefore, it is highly desirable to use heuristic techniques to reduce the complexity of designing the logic of the NGs' real-time decision-making systems.

3 | OVERVIEW OF THE CASE STUDY SYSTEM

As seen in Figure 4, the islanded DC MG is considered as a cluster of DC NGs (i.e. an MNG system) with a ring topology[1] architecture. The structure of a single NG is also shown in Figure 5. The NG contains a GW unit, a PV unit, a BESS, and a group of AC and DC CPLs. In this paper, NGs are

[1] The ring topology architecture is not a necessary requirement in this work. The DC MG can have any other single-bus topologies.

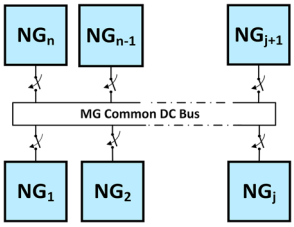

FIGURE 4 The islanded DC MG consisting of a cluster of NGs with ring topology architecture

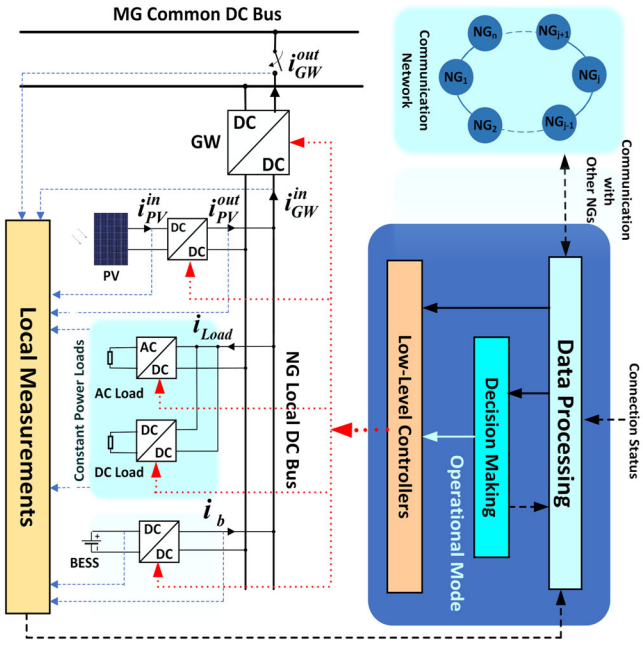

FIGURE 5 The schematic model of a DC NG in this work

designed as intelligent reactive agents that can change their dynamic behaviour and control objectives upon satisfying a predefined condition. Here, every single NG has a control unit containing two levels of controllers and a data-processing module. The data-processing module (see Figure 5) receives internal data from local measurements and external data through communication with neighbouring NGs. The higher-level controller is a decision-making module (i.e. a supervisory controller). This module is responsible for identifying the operational mode of NG (e.g. MG voltage control, SoC balancing etc.) and helps with avoiding SoC violation in BESSs, maximizing the PV power generation, and providing PnP capability for NGs. The lower level contains a group of controllers that compute references for the current regulators of power electronic converters to achieve the system objective at each operating mode. The NG control system is discussed in what follows.

4 | NGS' DECISION-MAKING MODULE

To increase the flexibility and adaptability of the system, each NG is designed as an intelligent reactive agent that can change the dynamic behaviour of its components (e.g. control objective, communication, or electrical connection) with respect to the system conditions. To this end, a discrete-event supervisory controller (i.e. decision-making module) is designed for each DC NG that selects the operational mode of the NG subsystems (e.g. PV, GW, BESS, load) based on predefined rules.

4.1 | Communication and GW module sequence of actions

Let assume an NG (e.g. NG_j) has two neighbouring NGs (e.g. NG_{j-1}, NG_{j+1}) that can share some information with them. The external inputs that NG_j receives from its neighbours are defined as

$$U_j = \{y_{(j-1,j)}, y_{(j+1,j)}, m_{j-1}^{GW}, m_{j+1}^{GW}\} \tag{2}$$

where $y_{(j-1,j)}$ and $y_{(j+1,j)}$ are the output signals of NG_{j-1} and NG_{j+1} sent to NG_j. m_{j-1}^{GW} and m_{j+1}^{GW} also represent the operating mode of the GW of the neighbouring NGs. The output signals of the NG_j are also defined as

$$Y_j = \{y_{(j,j-1)}, y_{(j,j+1)}, m_j^{GW}\} \tag{3}$$

where $y_{(j,j-1)}$ and $y_{(j,j+1)}$ are the signals sent by NG_j to NG_{j-1} and NG_{j+1}, respectively. m_j^{GW} is also the operating mode of the GW in NG_j. The NG sends its consensus protocol state (i.e. ψ_j) to the neighbouring NGs when its GW is in MG voltage control mode (i.e. $y_{(j,j-1)} = y_{(j,j+1)} = \psi_j$). In this operating mode, the GW operates as a MG grid-forming unit and regulates the MG common DC bus voltage. Once the GW module of the NG leaves this mode of operation, the NG passes the output signals of its neighbouring agents to each other (i.e. $y_{(j,j-1)} = y_{(j+1,j)}, y_{(j,j+1)} = y_{(j-1,j)}$). So, the output signals of the NG depend on the operational mode of the GW converter. It will be shown in Section 5 that by implementing this smart switching communication technique, the consensus protocols' value (i.e. ψ_j^*) becomes always equal to the average SoC of the BESSs in NGs whose GW is in MG voltage control mode (i.e. grid-forming NGs) regardless of the operating mode of NGs. Additionally, S represents the connection status of the NG, with '0' denoting isolated mode and '1' denoting MG-connected mode. When NG becomes islanded (i.e. $S = 0$), GW switches to the idle mode. In addition, to return to the grid-forming mode (i.e. MG voltage control mode), the GW first switches to a transient operational mode (i.e. battery charging or discharging) and operates as a grid following unit to charge/discharge the battery and reduce the difference between the BESS's SoC and the consensus value (i.e. $|SoC_j - \psi_j^*|$). Once this value becomes very small (i.e. less than 0.01), the GW module returns to the MG voltage control mode. It will be discussed later that this strategy is essential to maintain the smooth PnP operation of the NGs. In addition, to guarantee that at least half of the NGs which are connected to the MG common DC bus operate

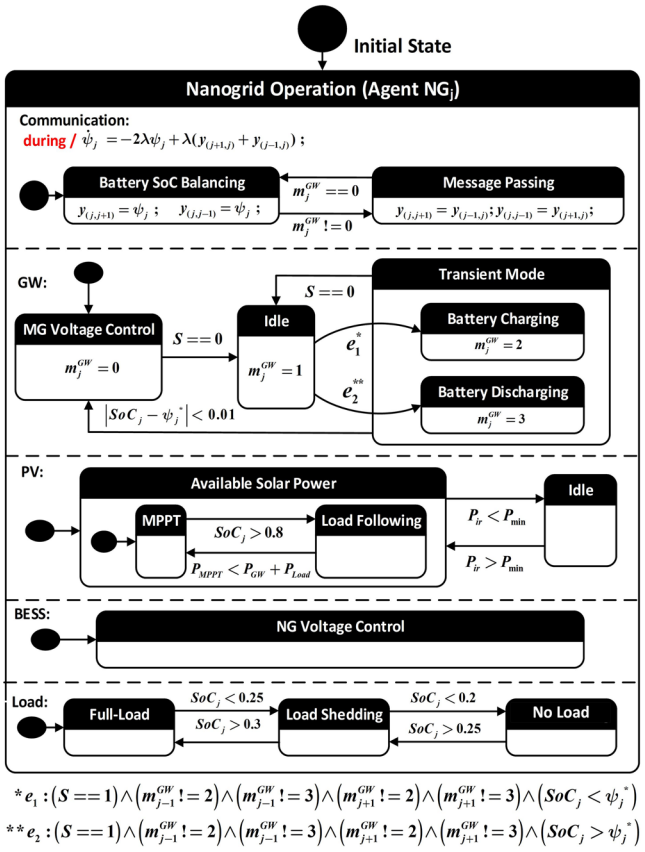

FIGURE 6 UML state diagram of the decision-making module. UML, unified modelling language.

as MG grid-forming units[2], NG_j cannot switch to the transient modes (i.e. battery charging or discharging) if its neighbouring NGs are in a transient mode (see e_1 and e_2 in Figure 6).

4.2 | PV, BESS, and load sequence of actions

The proposed logic can accommodate maximum PV power generation in the NGs. As seen in Figure 6, the PV unit *only* leaves the MPPT mode to balance the PV power generation and load *if* there is no capacity to store the extra generated power. This can occur when the NG_j is isolated, and its BESS is fully charged or NG_j is connected to the MG common DC bus and all the BESS of the MG grid-forming NGs are fully charged. The latter can be recognized by an individual NG since the power-sharing strategy among NGs proposed in Section 5.2 provides the same SoC value for all the BESSs in NGs whose GW is in MG voltage control mode (i.e. MG grid-forming units). Moreover, when the SoC of BESS becomes lower than a specific value (i.e. $SoC_j < 0.25$) the load unit switches to the load shedding mode by disconnecting the non-critical loads. If the load shedding action is not sufficient for maintaining the SoC of BESS higher than a minimum threshold value (i.e. $SoC_j < 0.20$), to maintain the system's stability the loads are disconnected and the system switches to the recovery (i.e. no load) mode to charge the batteries.

[2] MG grid-forming units (or grid-forming NGs) are the NGs whose GW converter regulates the MG common DC bus voltage.

4.3 | Evaluating the complexity and flexibility of the decision logic

As discussed in the previous section, the UML-based logic design provides a framework that can capture the concurrent behaviour of the NG components including communication system, GW, BESS, PV, and loads. Therefore, it intrinsically supports the process of the system states and switching conditions in a parallel manner, so that it facilitates the design of the supervisory controller. It can be easily shown that under the proposed method, each NG may react to the system changes by performing 72 different operating modes representing a high flexibility and adaptability of the NG control systems. To design this logic in the UML framework, it is just needed to define 13 substates for NG components which includes three substates for loads, three substates for PV, a single substate for BESS, four substates for GW, and two substates for the communication system. However, in the case of designing this logic with classical sequential frameworks such as finite state machines (FSMs) or state-flow charts, it is required to define 72 states which are equal to the number of operating modes of the NGs. In addition, to design and represent the proposed logic in classical FSMs it is needed to define 160 state transitions while the proposed UML method just requires defining 15 state transitions. Moreover, due to the modular representation of states, the UML methods support distributed or parallel execution of states, thereby increasing the scalability of the supervisory controller. Table 3 summarizes the advantages of the proposed UML strategy over the classical FSM methods.

5 | LOW-LEVEL CONTROLLERS

The low-level controllers of the NGs calculate reference values for the current regulators of the converters to achieve the system objectives at each operating mode. In the following, first, the proposed control strategies in PV and BESS are discussed. Then, the control structure of GW unit is proposed.

5.1 | PV and BESS control systems

As discussed in Section 4, the BESS is responsible for regulating the voltage of the NG local DC bus. From the NG local DC bus side, the other units (i.e. PV, load, and GW) operate as a CPL or a CPS according to the direction of their output current. Without loss of generality, it is assumed that BESS utilizes a bidirectional DC–DC buck converter. Figure 7 shows the circuit

TABLE 3 Comparing the proposed UML-based logic design with its equivalent FSM framework.[a]

Framework	Processing method	State definition	N_T[b]	N_S[c]
FSM	Sequential	Single layer, unscalable	160	72
UML	Parallel–concurrent computation	Hierarchical, modular, and scalable	15	13

[a]Each NG may perform 72 different operational modes under the proposed rule-based supervisory controller (in both FSM and UML).
[b]N_T is the total number of state-transition required to represent/implement the logic of the supervisory controller in each framework.
[c]N_S is the total number of substates required to represent/implement the logic of the supervisory controller in each framework.

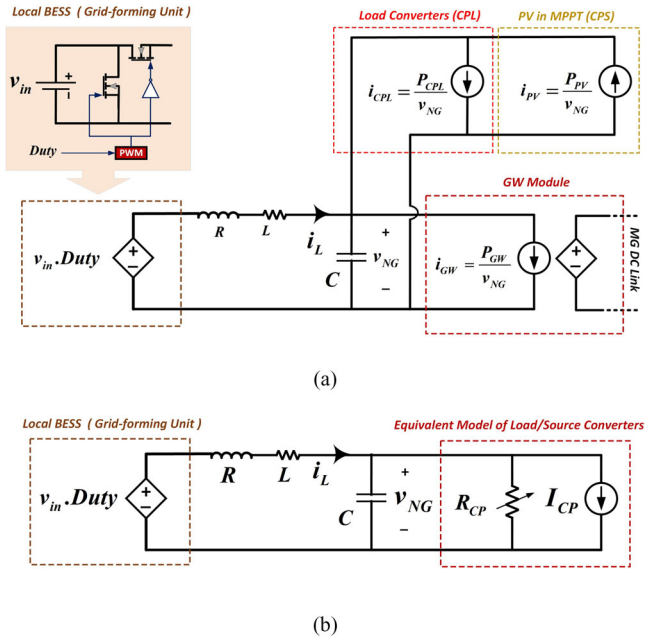

FIGURE 7 (a) The averaged dynamic circuit model of an NG local DC bus; (b) BESS and load/source converters replaced by their equivalent model at a given operating mode. (R, L, and C are the resistance, inductance, and capacitance of the converter's output filter, respectively)

model of the NG forms the point of view of BESS power electronic converter (i.e. the local grid-forming unit) that is adopted from [36]. In this model, only the averaged dynamics are considered, and the high frequency switching dynamics are ignored. In addition, the impedance of the NG DC link is neglected. The overall current of the parallel connected load/source converters in an NG (i.e. PV, load, and GW) is represented by i_o that is obtained as

$$i_{\mathrm{o}} = \frac{P_{\mathrm{CP}}}{v_{\mathrm{NG}}} \tag{4}$$

where P_{CP} is the total power of the constant power units (i.e. load/source converters) and it is obtained as

$$P_{\mathrm{CP}} = P_{\mathrm{GW}} + P_{\mathrm{Load}} - P_{\mathrm{PV}} \tag{5}$$

where P_{Load}, P_{PV}, and $P_{\mathrm{GW}}^{\mathrm{in}}$ are the power of the load, PV, and GW units at a given operating point, respectively. Thus, if $P_{\mathrm{CP}} < 0$, the buck converter is supplied by a CPS. Alternatively, if $P_{\mathrm{CP}} > 0$, the power electronic converter is loaded by a CPL that can cause some stability issues due to the negative incremental impedance of CPLs [28]. The equivalent linearized model of the constant power units at a given operating point can be also obtained as

$$i_{\mathrm{o}} = \left(-\frac{P_{\mathrm{CP}}}{V_{\mathrm{NG}}^2}\right) \times v_{\mathrm{NG}} + 2\frac{P_{\mathrm{CP}}}{V_{\mathrm{NG}}} \tag{6}$$

where V_{NG} is the voltage of NG DC bus at that given operating point. Equation (6) indicates that, at a given operating mode, the constant power units can be approximated by a resistance parallel with a constant current source as follows:

$$\begin{cases} I_{\mathrm{CP}} = 2\dfrac{P_{\mathrm{CP}}}{V_{\mathrm{NG}}} \\ R_{\mathrm{CP}} = -\dfrac{V_{\mathrm{NG}}^2}{P_{\mathrm{CP}}} \end{cases} \tag{7}$$

Figure 7b shows the equivalent circuit model of the NG. Therefore, the averaged dynamic model of the NG, at a given operating point, can be obtained as follows:

$$\begin{cases} L\dfrac{di_b}{dt} = v_{\mathrm{in}} \times \mathrm{Duty} - Ri_b - v_{\mathrm{NG}} \\ C\dfrac{dv_{\mathrm{NG}}}{dt} = i_b - \dfrac{v_{\mathrm{NG}}}{R_{\mathrm{CP}}} - I_{\mathrm{CP}} \end{cases} \tag{8}$$

where i_b is the output current of the BESS (see Figure 7) and v_{NG} is the voltage of the NG local DC bus. R, L, and C are also the resistance, inductance, and capacitance of the converter's output filter, respectively. Figure 8 shows the control structure of the BESS unit. To regulate the voltage of the NG local DC bus (i.e. v_{NG}), an AMPC algorithm is employed to compute a reference signal (i.e. i_{ref}) for the current regulator of the DC–DC converter of the BESS unit. The current regulator is a PI controller that calculates the duty cycle (i.e. Duty) of the converter to regulate its output current (i.e. i_b) to the reference value (i.e. i_{ref}). By adding the dynamics of the current regulator to Equation (8) and defining $\mathrm{Duty} = k_{\mathrm{p}}(i_{\mathrm{ref}} - i_b) +$

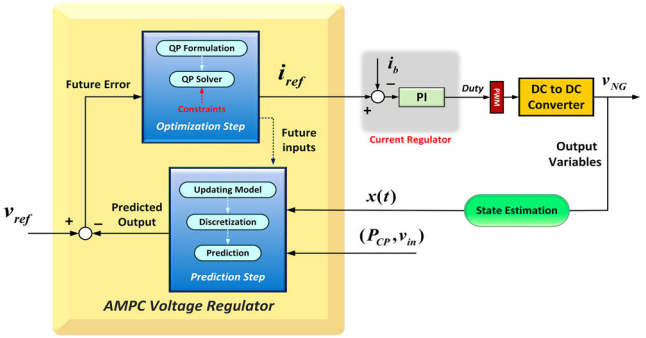

FIGURE 8 Block diagram of the BESS control system (i.e. the proposed NG local DC bus voltage control system). BESS, battery energy storage system.

$k_i \int (i_{ref} - i_b)dt$[3], where k_p and k_i are the proportional and integral gain of the PI current regulator, the linear time varying (LTV) dynamic model of the NG can be obtained in a state space form as

$$\begin{cases} \dot{x}(t) = A(t)x(t) + B(t)u(t) \\ y(t) = Cx(t) \end{cases} \tag{9}$$

where $x = [i_b, v_{NG}, e_{int}]^T$, $u = [u_{mv}\ u_{md}]^T$. e_{int} is defined as the integral of the error (i.e. $e_{int} = \int (i_{ref} - i_b)dt$). Also, $u_{mv}(t) = i_{ref}$ is the control input (or manipulated variable) and $u_{md}(t) = I_{CP}$ is the measured disturbance. A, B, and C are defined as

$$A = \begin{bmatrix} -\left(R + k_p v_{in}(t)\right)/L & -1/L & k_i v_{in}(t)/L \\ 1/C & -1/\left(R_{CP}(t)C\right) & 0 \\ -1 & 0 & 0 \end{bmatrix} \tag{10}$$

$$B = \begin{bmatrix} k_p v_{in}(t)/L & 0 \\ 0 & -1/C \\ 1 & 0 \end{bmatrix} \tag{11}$$

$$C = [0\ 1\ 0] \tag{12}$$

As seen, the NG system has a time-varying dynamic behaviour. Specially, the P_{CP} (or R_{CP}) may vary in a wide range during the NG operation. Consequently, the typical MPC techniques that employ the linear time invariant (LTI) approximation of the system cannot achieve the desired operation of the NG due to the inaccurate prediction model. However, AMPC control techniques have an interesting feature which is updating the prediction model at each control interval. As a result, the LTI approximation of the system at each control interval is more accurate. Also, AMPC is intrinsically a discrete-time controller. So, the AMPC requires a discrete-time approximation of the system (e.g. a discrete-time predictive model). Consequently, after updating the model parameters (e.g. R_{CP}, v_{in}) at each control interval, the AMPC controller utilizes the following discrete-time approximation of the system:

$$\begin{cases} x_d(k+1) = A_d x_d(k) + B_d u_d(k) \\ y_d(k) = C x_d(k) \end{cases} \tag{13}$$

where x_d, $u_d = [u_{dmv}\ u_{dmd}]^T$, and $y_d$are discrete time approximation of the system states, inputs, and output, respectively. Also, A_d and B_d are directly computed as

$$A_d = e^{AT_s}, B_d = \left(\int_{\tau=0}^{T_s} e^{A\tau} d\tau\right) B = A^{-1}\left(A_d - I\right) B \tag{14}$$

where T_s is the AMPC sampling time. Then, the AMPC algorithm solves a quadratic programming (QP) formulation using an active set optimization method to compute the sequence of future control actions (i.e. the reference current). To this end, it minimizes the following cost function, at each time step (i.e. k):

$$\begin{aligned} J = &\sum_{i=1}^{H_p} \eta_e \left(v_{ref}(k+i|k) - y_d(k+i|k)\right)^2 \\ &+ \sum_{i=1}^{H_c} \eta_c \left(u_{dmv}(k+i|k) - u_{dmv}(k+i-1|k)\right)^2 \end{aligned} \tag{15}$$

subject to

$$-i_b^{nom} \le \frac{u_d(k+i|k)}{1.1} \le i_b^{nom}, i \in \{1, \ldots, H_c\} \tag{16}$$

where H_p and H_c are the prediction and control horizon and $H_c < H_p$. v_{ref} is the reference voltage and $\forall k, v_{ref}(k) = v_{nom}$. $u_{dmv}$is the manipulated variable and$u_{dmv}(k) = i_{ref}(k)$. η_e and η_c are also the weights of the error and manipulated variable move, respectively. So, by adjusting η_e/η_c, one can provide an optimal tradeoff between voltage regulation of the NG local DC bus and current ripples of the BESS. Finally, after computing the sequence of future control actions, the AMPC imposes the first one and goes for the next time step.

As seen, the proposed AMPC controller indirectly regulates the output voltage of the BESS converter (or NG local DC bus voltage) by calculating a reference trajectory for its lower-hand PI current regulator. This structure is relatively similar to the conventional NG control strategies in which a PI voltage controller computes a reference value for its cascaded PI current regulator. Therefore, the AMPC control interval (or sampling time) can be similar to the sampling time of conventional PI voltage regulators in NG applications which is in the range of a

[3] In practice, the current regulator is a digital controller that has a much lower sampling time than its higher-level discrete-time NG voltage regulator. So, from the NG voltage controller point of view, it can be approximated by a continuous-time system.

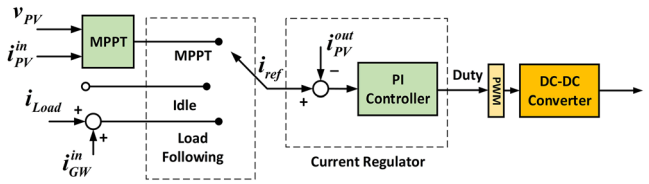

FIGURE 9 Block diagram of the PV control system. PV, photovoltaic.

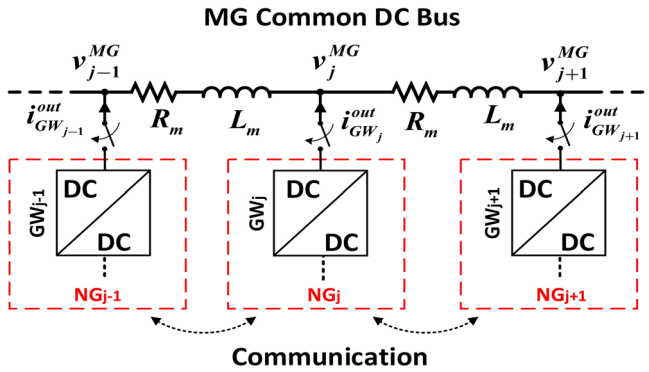

FIGURE 10 The structure of the parallel connected NGs in the DC MG system

millisecond. However, the conventional direct MPC techniques (e.g. FCS-MPC) typically require a sampling time in the range of a few microseconds. Thus, the direct MPC methods should carry out approximately the same number of computations in a significantly shorter time frame compared to the proposed AMPC technique. Hence, in terms of hardware requirements, the proposed approach is considerably less demanding than the direct MPC methods and it may be more comparable with the conventional NG PI voltage controllers. In addition, the proposed approach maintains the structure of the conventional NG voltage control systems (i.e. two cascaded controllers and a PWM). Consequently, the implementation of this technique does not require a major restructuring of the conventional NG voltage control system.

Figure 9 shows the control structure of the PV unit. The PV unit has three different operating modes including an MPPT, an idle, and a load following mode. During the load following mode, the output power of the PV is approximately equal to the demanded power by the GW and load (i.e. $P_{\mathrm{PV}} \simeq P_{\mathrm{GW}}^{\mathrm{in}} + P_{\mathrm{Load}}$). Thus, when PV switches to this mode, the output current of the BESS becomes nearly zero to avoid battery SoC violation. In addition, the PV module will switch to the idle mode if the available solar irradiance power becomes less than a threshold value (i.e. $P_{\mathrm{ir}} < P_{\mathrm{min}}$).

5.2 | GW control systems

The GW converter of an NG has four different operating modes including an MG voltage control (i.e. MG grid-forming mode), two transient modes, and an idle mode. Figure 10 illustrates the structure of the parallel connected NGs in the MNG system where v_j^{MG} and $i_{\mathrm{GW}_j}^{\mathrm{out}}$ are the output voltage and current of the NG_j .R_m and L_m are also resistance and inductance of the DC link between two neighbouring NGs. During the MG voltage control mode, the NGs communicate with each other based on a consensus protocol to regulate the voltage of the MG common DC bus (i.e. v_j^{MG}) as well as sharing power. In this approach, all the grid-forming NGs balance the SoC of their BESS unit with each other. The agents (i.e. NGs) have an undirected ring communication network topology illustrated in Figure 11a. Define $\mathcal{A}$ as the set of all agents, and $\mathcal{A}_G \subseteq \mathcal{A}$as the set of grid-forming NGs. Also, consider N_j as the set of neighbours of NG_j that can be obtained as

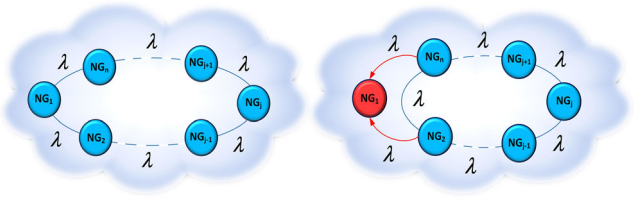

FIGURE 11 Adaptive communication network topology of NGs. (a) All the NGs operate the battery SoC balancing mode (i.e. all the GW modules are in MG voltage control mode), (b) an NG (e.g. NG1) switches to the message passing mode. SoC, state of charge.

$$N_j = \begin{cases} \{n, 2\}, j = 1 \\ \{j-1, j+1\}, 2 \le j \le n-1 \\ \{n-1, 1\}, j = n \end{cases} \tag{17}$$

So, $\forall j \in \mathcal{A}$, the number of elements in $N_j$is two (i.e. $|N_j| = 2$). The protocol state of the NG_j (i.e. ψ_j) is defined as follows:

$$\dot{\psi}_j(t) = -2\lambda\psi_j + \lambda \sum_{i \in N_j} y(i, j) \tag{18}$$

where $y(i, j)$ is the output signal of the NG_i sent to the NG_j, and λ is the gain of communication network.

First, assume that all the GW units are in the MG voltage control mode (i.e. $\mathcal{A}_G = \mathcal{A}$). As discussed in Section 4, when the GW unit of NG_j is in grid-forming mode, it sends its protocol state to the neighbouring agents (i.e. $y(j, i) = \psi_j, i \in N_j$). Consequently, $\forall j \in \mathcal{A}$, (18) is reformulated as

$$\dot{\psi}_j(t) = -2\lambda\psi_j + \lambda \sum_{i \in N_j} \psi_i \tag{19}$$

Equation (19) can be represented in the state space form as

$$\dot{\psi}(t) = -L\psi(t) \tag{20}$$

where $\psi = [\psi_1, \psi_2 \ldots, \psi_n]^T$ and $L = [l_{ji}]_{n\times n}$ is the graph Laplacian matrix of the network that is obtained as

$$l_{ji} = \begin{cases} -\lambda, i \in N_j \\ 2\lambda, i = j \end{cases} \quad (21)$$

Equations (19) to (21) represent a standard static averaging consensus algorithm. By reinitializing $\psi_j(0) = SoC_j(kT'_s)$ at each sampling time (i.e. k), it can be shown if λ is enough large, all the protocol states will converge to a consensus value [37] (i.e. $\forall j \in \mathcal{A}, \psi_j^* = SoC^*$) that is obtained as

$$SoC^* = \frac{1}{|\mathcal{A}|}\sum_{j\in\mathcal{A}} SoC_j(kT'_s) = \frac{1}{n}\sum_{j=1}^{n} SoC_j(kT'_s) \quad (22)$$

where $|\mathcal{A}| = n$ is the total number of NGs and T'_s is the sampling period. So, if $\mathcal{A}_G = \mathcal{A}$ and λ is enough large, the steady-state values of protocol states at each sampling period (i.e. ψ_j^*) are equal to the average SoC of all BESSs.

Now, assume that an NG (e.g. NG_1) switches to one of the transient or idle modes (i.e. $\mathcal{A}_G = \mathcal{A} - \{1\}$). So, the communication module of NG_1 switches to the message passing mode (see Figure 6). In this case, NG_1 passes the outputs of its neighbouring agents (i.e. $\{n, 2\} \in N_1$) to each other (i.e. $y(1,2) = \psi_n, y(1,n) = \psi_2$). Figure 11b shows the equivalent communication network when NG_1 is in the message passing mode. In this case, the protocol states can be obtained as

$$\dot{\psi}(t) = -L'\psi(t) \quad (23)$$

where the new Laplacian matrix, L', is obtained as

$$L' = \begin{bmatrix} 2\lambda & -\lambda & 0 & \ldots & -\lambda \\ 0 & & & & \\ \vdots & & [l'_{ji\in\mathcal{A}_G}] & & \\ 0 & & & & \end{bmatrix}_{n\times n} \quad (24)$$

where $\forall ij \in \mathcal{A}_G, l'_{ji} = l'_{ij}$ and $\sum_{i\in\mathcal{A}_G} l'_{ji} = 0$. Thus, by reinitializing $\psi_j(0) = SoC_j(kT'_s)$ at each sampling time, the protocol states of all the MG grid-forming units converge to a consensus value (i.e. $\forall j \in \mathcal{A}_G, \psi_j^* = SoC^*$) that is obtained as follows:

$$SoC^* = \frac{1}{|\mathcal{A}_G|}\sum_{j\in\mathcal{A}_G} SoC_j(kT'_s) = \frac{1}{n-1}\sum_{j=2}^{n} SoC_j(kT'_s) \quad (25)$$

where $|\mathcal{A}_G| = n - 1$ is the total number of grid-forming NGs. Also, based on (24), ψ_1^* is obtained as

$$\psi_1^* = \frac{1}{2}\sum_{j\in N_1}\psi_j^* = \frac{\psi_2^* + \psi_n^*}{2} = SoC^* \quad (26)$$

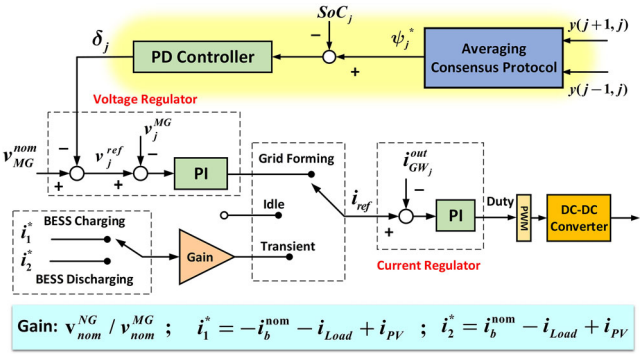

FIGURE 12 Block diagram of the GW control system in a DC NG (e.g. NG_j)

So, based on the proposed approach, the protocol states of all NGs always reach a consensus value that is equal to the average SoC of all the batteries in the grid-forming NGs regardless of the NGs operating mode. This can be represented as follows:

$$\forall j \in \mathcal{A}, \psi_j^* = \frac{1}{|\mathcal{A}_G|}\sum_{j\in\mathcal{A}_G} SoC_j(kT'_s) \quad (27)$$

ψ_j^* is then used by the GW units of the NGs to balance the SoC of the BESSs with each other.

Figure 12 shows the control structure of the GW module in NG_j. When the GW is in the MG voltage control mode, it measures the error between the SoC of its BESS and the average SoC of all the grid-forming units (i.e. ψ_j^*) and then sends the error to the proportional derivative (PD) controller. In this case, if the error (i.e. $\psi_j^* - SoC_j$) increases, the PD controller slightly reduces the voltage reference of the GW module (i.e. v_j^{ref}) to deliver more electrical power to the NG and charges the battery. On the other hand, if the SoC of BESS becomes higher than the average SoC of the grid-forming NGs, the outputs of the PD controller (i.e. δ_j) decrease to increase the output power of the NG and discharge the battery. It will be shown in Section 6 that this technique can balance the SoC of the BESSs in all grid-forming units. In addition, when NG is isolated, the GW module switches to the idle mode and delivers no power. In this mode, the NG cannot balance the SoC of BESS with other NGs. Thus, if the NG directly switches from the isolated mode to the MG voltage control mode, the error between the consensus value and SoC of BESS (i.e. $\psi_j^* - SoC_j$) will be large. Consequently, the PD controller's output may be very large (i.e. $|\delta_j| \gg 0$) that can cause a significant voltage deviation on the MG common DC bus. In addition, it may deliver a significant power to the NG which may destabilize the system. To improve the PnP ability of the NGs and provide a bump less transition to the grid-forming mode, the NG first switches to a transient mode (see the internal logic of NGs in Figure 6). In the transient mode, the GW operates as a grid following unit and delivers power to the NG that charges/discharges the BESS with its nominal value (i.e. i_b^{nom}). Once the error becomes very low (i.e. $|\psi_j^* - SoC_j| \leq 0.01$) the GW switches to the MG voltage control mode. It should be noted there is not any community load

TABLE 4 System parameters

Symbol	DESCRIPTION	Value
$v_{\text{nom}}^{\text{NG}}$	Nominal voltage of NGs' DC bus	100 V
$v_{\text{nom}}^{\text{MG}}$	Nominal voltage at MG DC bus	750 V
i_b^{nom}	Nominal output current of the BESSs	100 A
Q	Nominal charge time of the batteries	3 h
$P_{\text{load}}^{\text{nom}}$	Nominal load power at each NG	10 kW
$P_{\text{PV}}^{\text{nom}}$	Nominal PV power generation	10 kW
P_b^{nom}	Nominal power of BESS	10 kW
λ	Gain of communication network	5
k_{P}^{PD}	Proportional gain of the PD controller	400
k_{d}^{PD}	Derivative gain of the PD controller	10
N_d	Filter coefficient of the PD controller	1
R_m	Resistance of the MG DC link	10mΩ
L_m	Inductance of the MG DC link	5mH
k_p^C	Proportional gain of current regulator	0.8
k_i^C	Integral gain of current regulator	4
k_p^V	Proportional gain of voltage regulator	4
k_i^V	Integral gain of voltage regulator	50
T_s	AMPC controllers. sampling time	1 ms
H_p	Prediction horizon of AMPC	10
H_c	Control horizon of AMPC	2
η_e	Weight of error minimization	0.75
η_c	Weight of manipulated variable move	0.066

or CPL on the MG common DC link, so the conventional cascaded PI controllers can provide a good voltage regulation at MG common DC link.

In conclusion, the system computes the average SoC of all the batteries that are in grid-forming NGs using a switching averaging consensus protocol regardless of the NGs' operating mode representing a high-level flexibility. The consensus value is then used as a reference SoC by the GW module of the MG grid-forming units to balance the SoC of their batteries with each other. The consensus value is also used by the supervisory controllers of all units to select the operational mode of the system and ensure the safe automatic connection of the NGs to the MG common DC bus. It will be shown in Section 6 that the proposed adaptive distributed power-sharing technique can accurately balance the SoC of the BESS in different NGs while maintaining the PnP ability of NGs.

6 | SIMULATION RESULTS

The performance of the proposed control system is evaluated by simulating a test system using MATLAB/Simulink. The test system is an islanded MNG which consists of four similar DC NGs. The BESSs are also similar, and they are lithium-ion type. The system parameters are illustrated in Table 4.

6.1 | AMPC performance evaluation

Figure 13 illustrates the performance of the proposed AMPC technique compared to a conventional NG voltage control system (i.e. a regular PI voltage controller represented in Figure 2). It is believed that this comparison is reasonable because both control systems have the same structure in which the voltage controllers (i.e. AMPC and PI) calculate a reference signal for the current regulator of the bidirectional DC–DC converter (i.e. the current controller of the BESS unit). They also have a similar saturation limit that is equal to $1.1i_b^{\text{nom}}$(i.e. $|i_{\text{ref}}| < 1.1i_b^{\text{nom}}$) and a same sampling time (i.e. $T_s = 1$ ms). In addition, they utilize an exactly similar PWM technique and use similar converter output filters. To consider the operational saturation limits, the PI voltage controller uses a back calculation anti-windup technique. On the other hand, the AMPC minimizes the proposed cost function in (15) subject to the saturation constraint (see (15) and (16)). As discussed before, P_{CP} represents the total power of the constant power units that is defined in (5). If $P_{\text{CP}} > 0$, the DC–DC converter of the BESS unit will supply a CPL that can provide some stability concerns caused by the negative incremental impedance of CPLs [1, 22]. In the case study system, the maximum CPL is 10 kW (i.e. $|P_{\text{CP}}| < 10$ kW). Figure 13a represents the variation of P_{CP} in the test system. Figure 13b shows the transient voltage variation of the NG local DC bus during P_{CP} changes. The conventional PI controller causes more voltage variation on the NG local DC bus compared to the proposed AMPC technique. Particularly, at maximum CPL (i.e. $t \in T_1$), the PI controller has a small marginal stability that causes a poor transient response and significant voltage oscillation on the NG local DC bus. Figure 13b also shows that in higher CPL values, the system experiences significantly worse transient response in the PI voltage control technique, while the AMPC performance is not affected by the large CPL values. Figure 13c represents the output current of the BESS in both control techniques. The AMPC provides fewer current ripples compared to the PI controller. So, due to the limited life cycle of the BESSs, the AMPC algorithm can also increase the efficiency of the system by increasing the lifetime of the BESSs. In conclusion, the proposed AMPC approach considerably overperformed the regular PI voltage controller results in more reliability (i.e. better voltage regulation) and more efficiency (i.e. increasing the lifetime of the BESSs).

6.2 | Battery SoC balancing (power sharing)

The battery SoC balancing performance of the proposed approach is studied in this section. The net power is defined as the difference between generation power and load consumption in each NG (i.e. $P_{\text{net}} = P_{\text{PV}} - P_{\text{Load}}$). Figure 14 shows the so-called net power profiles in the DC MG system during the 5-h simulation interval. The PV power generation in NG_2 is higher than the load consumption (i.e. $P_{\text{PV}} > P_{\text{Load}}$), while the net power in the other NGs has a negative value. Figure 15 illustrates the SoC of BESSs in two different scenarios. In both

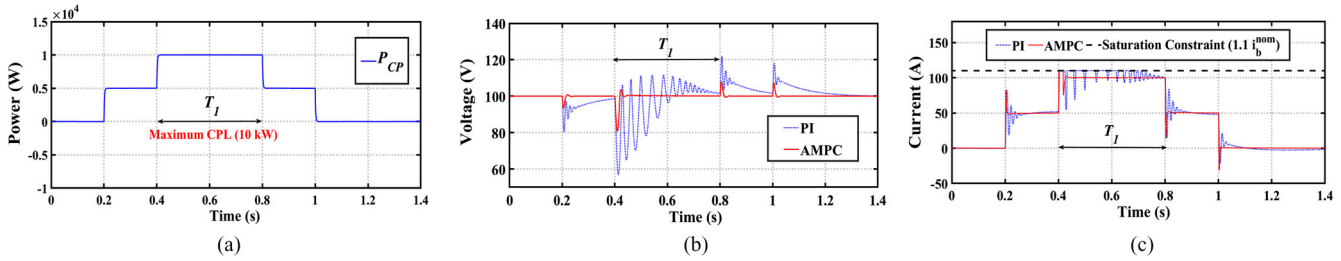

FIGURE 13 The performance of the proposed AMPC technique compared to a PI voltage controller: (a) CPP changes, (b) voltage variation of the NG local DC bus, (c) output current of the BESS (i.e. bi)

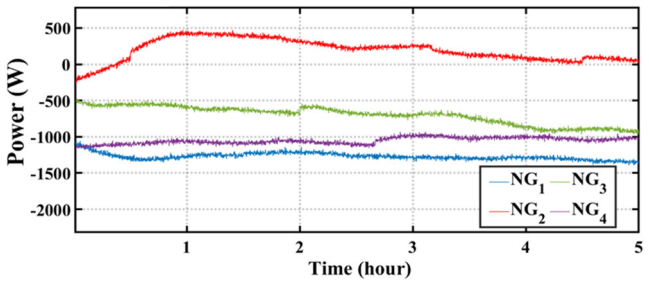

FIGURE 14 The net power profile in different NGs during the simulation interval

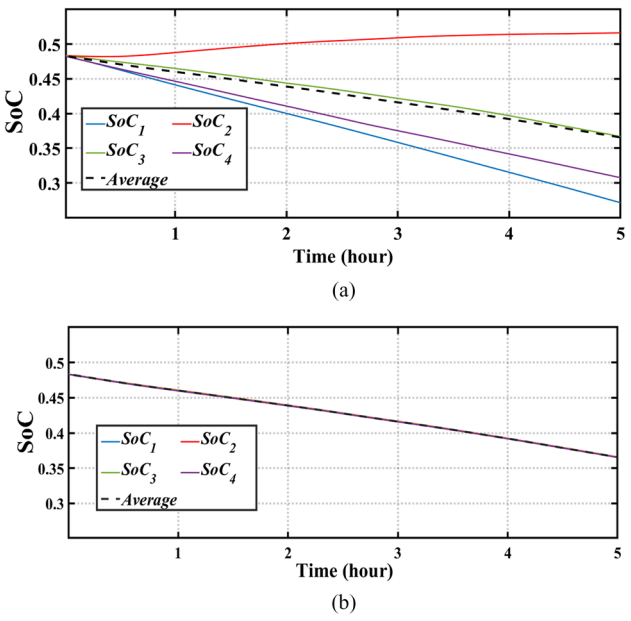

FIGURE 15 Battery SoC balancing performance of the proposed approach. (a) First scenario, (b) second scenario

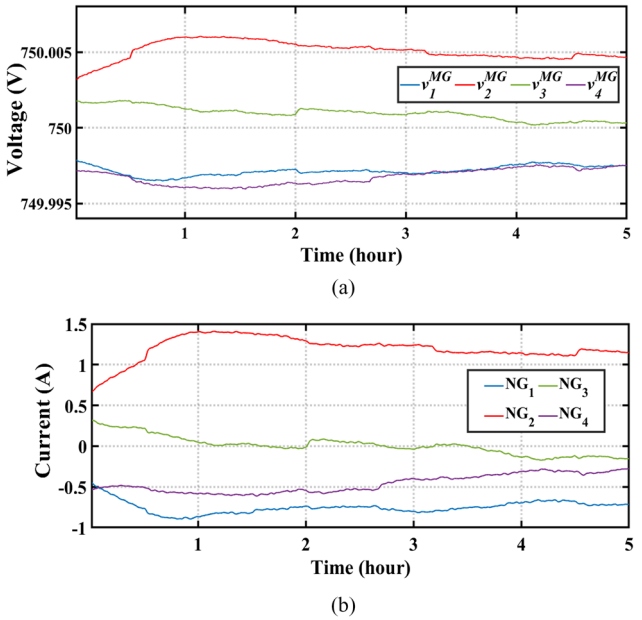

FIGURE 16 Voltage and current variations in MG common DC bus. (a) Output voltages of GW converters, (b) output currents of GW converters

scenarios, all the NGs initially have a same SoC value. In the first scenario, all the NGs are isolated and share no power with each other. In the second scenario, it is assumed that all the NGs are connected to the MG common DC bus and all the GW modules are in MG grid-forming mode (i.e. grid-forming NGs). Due to the similar power generation and load values (i.e. similar net power), the average SoC of BESSs in both scenarios are the same. However, as seen in Figure 15b, in the second scenario, the SoCs of all BESSs are balanced with each other that verifies the effectiveness of the distributed power-sharing approach. Consequently, the BESSs altogether behave similar to a cloud ESS (e.g. a community BESS). This BESS aggregation is highly beneficial that results in maximum utilization of BESSs capacities and increases the MNG reliability. Figure 16 also represents the voltage deviation of the MG DC common DC bus and the output current of the GW units (i.e. i_{GW}^{out}) under the proposed control approach (i.e. second scenario). As seen, the voltage deviation on MG common DC link is very low, and it can be negligible. Thus, the proposed distributed power-sharing method does not affect the voltage regulation of the MG common DC bus. However, the decentralized droop-based techniques usually generate 2% to 5% steady-state voltage deviations.

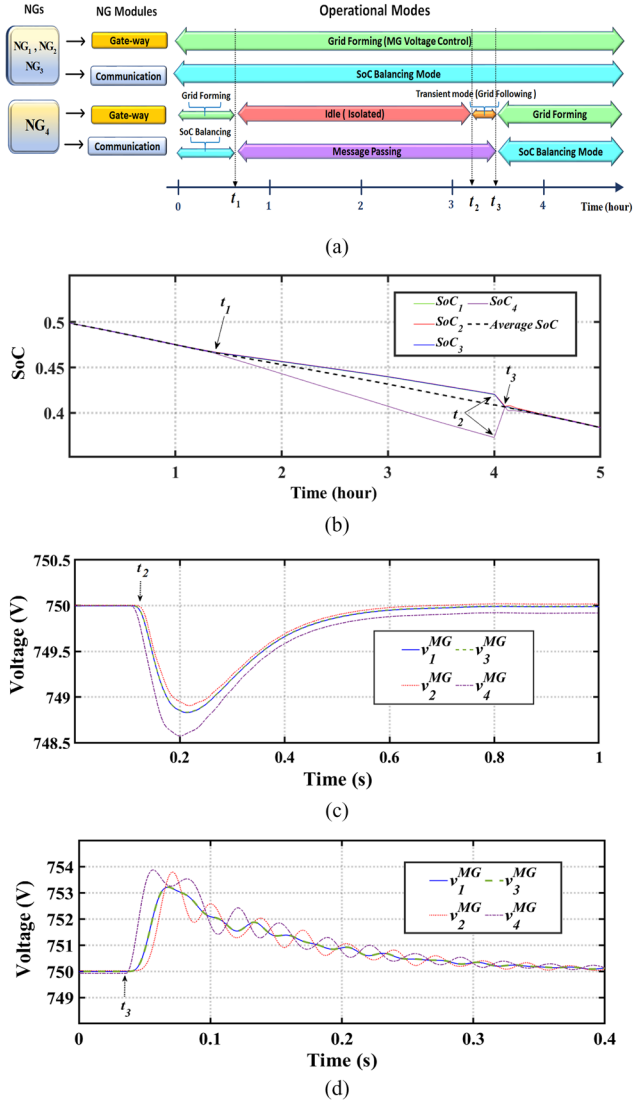

FIGURE 17 Plug and play operation of NG. (a) Sequence of actions, (b) SoC variation of the NGs, (c) voltage variation of MG common DC bus at t = t2, (d) voltage variation of MG common DC bus at t = t3

6.3 | PnP operation of NGs

This section investigates the PnP ability of the DC NGs. Figure 17a shows the sequence of actions in PnP operation of an NG. In this test case, all the NGs are initially connected to the MG common DC bus and all the GW units are in MG voltage control mode (i.e. grid-forming NGs[4]). In addition, the net power at each NG is like the test cases in Section 6.2. At $t = t_1$, NG_4 becomes isolated, and its GW module switches to the idle mode. During the isolated mode, NG_4 does not share power and its SoC value cannot be balanced with other NGs. In this mode, instead of its protocol state (i.e. ψ_4), NG_4 sends the protocol state of NG_3 (i.e. ψ_3) to NG_1 and ψ_1 to NG_3. Thus, the protocol states of all NGs converge to the average SoC of grid-forming NGs (i.e. NG_1, NG_2, and NG_3). Therefore, the grid-forming NGs balance their SoC value with each other. At $t = t_2$, the NG_4 becomes connected to the MG DC link. So, its GW module switches to the battery charging transient mode (i.e. grid following) to charge the BESS with its nominal power (i.e. i_b^{nom}) during $T = [t_2\ t_3]$ time interval. Since at $t = t_3$, the difference between the battery SoC and the consensus value (i.e. ψ_4^*) becomes very small (i.e. $|\psi_4^* - SoC_4| < 0.01$), the GW unit of NG_4 switches to the MG voltage control mode and balances the SoC of its BESS with other NGs. The SoC variation of all BESS is illustrated in Figure 17b.

The transient voltage variation on the MG common DC bus in t_2 and t_3 switching instances is also illustrated in Figures 17c and 17d, respectively. These voltage variations in both switching instances are insignificant compared to the nominal voltage of the MG common DC bus (i.e. 750 V). In conclusion, each NG can be isolated and then safely connected to MG common DC bus without any manual modification on the voltage control system and power-sharing algorithm, representing the PnP ability of the NGs.

7 | DISCUSSION

The proposed adaptive battery SoC balancing strategy provides the same SoC value for all the BESSs inside the MG. Consequently, the BESSs altogether behave like a community BESS or a cloud ESS whose capacity is equal to the summation of all the BESSs capacities. Consequently, the proposed approach can improve the overall efficiency of the system by utilizing the maximum energy storage capacity of batteries. Compared to the centralized cloud energy storages, the proposed distributed technique can enhance the resiliency and flexibility of the system by enabling the DC NGs to utilize their local BESS in the isolated mode. However, it may increase the initial cost of the system. Thus, based on the system objectives, further cost-benefit analysis should be applied to compare the centralized cloud energy storage technologies with the proposed distributed technique in different clustered NG applications.

8 | CONCLUSION

An adaptive multiagent-based control strategy is presented to provide effective and flexible voltage regulation and power sharing in an MNG system. The performance of the proposed approach is validated using MATLAB/Simulink. Each NG is designed as a reactive agent that has a hierarchical control system. The top level is a discrete-event supervisory controller that selects the operational mode of the agent based on predefined rules. The supervisory control layer ensures the PnP ability of the NGs as well as the effective operation of the system. The low-level controllers are responsible for power sharing and voltage regulation with respect to the operational mode of the agent. To regulate the voltage of the NGs local DC bus, an adaptive model predictive controller is deployed providing better transient response, and fewer current ripples compared to regular

[4] Remember that the grid-forming NGs (or MG grid-forming NGs) are those whose GW module regulates the MG common DC bus voltage.

PI voltage controllers. Additionally, a switching consensus control algorithm is presented that strongly regulates the voltage of MG common DC bus as well as offering accurate power sharing among the NGs by balancing the SoC of all BESS in different NGs while maintaining the PnP operation of them. Consequently, the proposed adaptive multi-agent control strategy provides effective cooperation of the clustered NGs as well as maintaining the scalability and flexibility of the system.

ACKNOWLEDGEMENTS

This paper is based upon work supported by the National Science Foundation EPSCoR Program under Award #OIA-1757207.

CONFLICT OF INTEREST

No.

DATA AVAILABILITY STATEMENT

The data that support the findings of this study are available from the corresponding author upon reasonable request.

REFERENCES

1. Xu, Q., Vafamand, N., Chen, L., Dragicevic, T., Xie, L., Blaabjerg, F.: Review on advanced control technologies for bidirectional DC/DC converters in DC microgrids. IEEE J. Emerg. Sel. Top. Power Electron. 9 (2), 1205–1221 (2020)
2. Nordman, B., Christensen, K.: Local power distribution with nanogrids. In: 2013 International Green Computation Conference Proceedings, IGCC 2013 (2013)
3. Burmester, D., Rayudu, R., Seah, W., Akinyele, D.: A review of nanogrid topologies and technologies. Renew. Sustain. Energy Rev. 67, 760–775 (2017)
4. Werth, A., Kitamura, N., Tanaka, K.: Conceptual study for open energy systems: Distributed energy network using interconnected DC nanogrids. IEEE Trans. Smart Grid 6 (4), 1621–1630 (2015)
5. Srinivasan, M., Kwasinski, A.: Control analysis of parallel DC-DC converters in a DC microgrid with constant power loads. Int. J. Electr. Power Energy Syst. 122, 106207 (2020)
6. Mosayebi, M., Gheisarnejad, M., Khooban, M.-H.: An intelligent type-2 fuzzy stabilization of multi-DC nano power grids. IEEE Trans. Emerg. Top. Comput. Intell. 1–6 (2020)
7. Nasir, M., Anees, M., Khan, H.A., Guerrero, J.M.: Dual-loop control strategy applied to the cluster of multiple nanogrids for rural electrification applications. IET Smart Grid 2 (3), 327–335 (2019)
8. Leonori, S., Rizzoni, G., Frattale Mascioli, F.M., Rizzi, A.: Intelligent energy flow management of a nanogrid fast charging station equipped with second life batteries. Int. J. Electr. Power Energy Syst. 127, 106602 (2021)
9. Tsikalakis, A.G., Hatziargyriou, N.D.: Centralized control for optimizing microgrids operation. In: IEEE Power and Energy Society General Meeting (2011)
10. Talapur, G.G., Suryawanshi, H.M.: A modified control scheme for power management in an AC microgrid with integration of multiple nanogrids. Electron. 8 (5), 1–14 (2019)
11. Nguyen, T.L., Griepentrog, G.: A self-sustained and flexible decentralized control strategy for DC nanogrids in remote areas/islands. In: Proceedings - 2017 IEEE Southern Power Electronics Conference, SPEC 2017. Institute of Electrical and Electronics Engineers Inc., pp. 1–6 (2018)
12. Mosayebi, M., Sadeghzadeh, S.M., Khooban, M.H., Guerrero, J.M.: Decentralised non-linear I–V droop control to improve current sharing and voltage restoration in DCNG clusters. IET Power Electron. 13 (2), 248–255 (2020)
13. Saad, A.A., Faddel, S., Mohammed, O.: A secured distributed control system for future interconnected smart grids. Appl. Energy 243 (January), 57–70 (2019)
14. Miao, Z., Xu, L., Disfani, V.R., Fan, L.: An SOC-based battery management system for microgrids. IEEE Trans. Smart Grid 5 (2), 966–973 (2014)
15. Li, C., Coelho, E.A.A., Dragicevic, T., Guerrero, J.M., Vasquez, J.C.: Multiagent-based distributed state of charge balancing control for distributed energy storage units in AC microgrids. IEEE Trans. Ind. Appl. 53 (3), 2369–2381 (2017)
16. Belal, E.K., Yehia, D.M., Azmy, A.M.: Adaptive droop control for balancing SOC of distributed batteries in DC microgrids. IET Gener. Transm. Distrib. 13 (20), 4667–4676 (2019)
17. Wu, Q., Guan, R., Sun, X., Wang, Y., Li, X.: SoC balancing strategy for multiple energy storage units with different capacities in islanded microgrids based on droop control. IEEE J. Emerg. Sel. Top. Power Electron. 6 (4), 1932–1941 (2018)
18. Nasir, M., Jin, Z., Khan, H.A., Zaffar, N.A., Vasquez, J.C., Guerrero, J.M.: A decentralized control architecture applied to DC nanogrid clusters for rural electrification in developing regions. IEEE Trans. Power Electron. 34 (2), 1773–1785 (2019)
19. Samende, C., Bhagavathy, S.M., McCulloch, M.: State of charge based droop control for coordinated power exchange in low voltage DC nanogrids. In: Proceedings of the International Conference on Power Electronics Drive System (2019)
20. Dragicevic, T., Lu, X., Vasquez, J.C., Guerrero, J.M.: DC Microgrids - Part I: A Review of Control Strategies and Stabilization Techniques. vol. 31, Institute of Electrical and Electronics Engineers Inc. pp. 4876–4891 (2016)
21. Yazdanian, M., Mehrizi-Sani, A.: Distributed control techniques in microgrids. IEEE Trans. Smart Grid 5 (6), 2901–2909 (2014)
22. Singh, S., Gautam, A.R., Fulwani, D.: Constant power loads and their effects in DC distributed power systems: A review. Renew. Sustain. Energy Rev. 72 (December 2015), 407–421 (2017)
23. AL-Nussairi, M.K., Bayindir, R., Padmanaban, S., Mihet-Popa, L., Siano, P.: Constant power loads (CPL) with microgrids: Problem definition, stability analysis and compensation techniques. Energies 10 (10), (2017)
24. Vafamand, N., Khayatian, A., Khooban, M.H.: Stabilisation and transient performance improvement of DC MGs with CPLs: Nonlinear reset control approach. IET Gener. Transm. Distrib. 13 (14), 3169–3176 (2019)
25. Du, W., Zheng, K., Wang, H.F.: Instability of a DC microgrid with constant power loads caused by modal proximity. IET Gener. Transm. Distrib. 14 (5), 774–785 (2020)
26. Ghorashi Khalil Abadi, S.A., Bidram, A.: A distributed rule-based power management strategy in a photovoltaic/hybrid energy storage based on an active compensation filtering technique. IET Renew. Power Gener. 15, 3688–3703 (2021)
27. Khodadoost Arani, A.A., Gharehpetian, B., Abedi, M.: Review on energy storage systems control methods in microgrids. Int. J. Electr. Power Energy Syst. 107, 745–757 (2019)
28. Karami, Z., Shafiee, Q., Khayat, Y., Yaribeygi, M., Dragicevic, T., Bevrani, H.: Decentralized model predictive control of DC microgrids with constant power load. IEEE J. Emerg. Sel. Top. Power Electron. 9(1), 451–460 (2019)
29. Long, B., Liao, Y., Chong, K.T., Rodriguez, J., Guerrero, J.M.: MPC-controlled virtual synchronous generator to enhance frequency and voltage dynamic performance in islanded microgrids. IEEE Trans. Smart Grid 12(2), 953–964 (2020)
30. Ghorashi Khalil Abadi, S.A., Habibi, S.I., Khalili, T., Bidram, A.: A model predictive control strategy for performance improvement of hybrid energy storage systems in DC microgrids. IEEE Access 10, 25400–25421 (2022)
31. Karamanakos, P., Liegmann, E., Geyer, T., Kennel, R.: Model predictive control of power electronic systems: methods, results, and challenges. IEEE Open J. Ind. Appl. 1, 95–114 (2020)

32. Zheng, C., Dragicevic, T., Blaabjerg, F.: Current-sensorless finite-set model predictive control for LC-Filtered voltage source inverters. IEEE Trans. Power Electron. 35 (1), 1086–1095 (2020)
33. Karamanakos, P., Geyer, T.: Guidelines for the design of finite control set model predictive controllers. IEEE Trans. Power Electron. 35 (7), 7434–7450 (2020)
34. Ebrahimian, A., Vahid, S., Weise, N., El-Refaie, A.: Two level AC-DC-AC converter design with a new approach to implement finite control set model predictive control. In: Proceedings of the IEEE International Conference on Industrial Technology. Institute of Electrical and Electronics Engineers Inc., pp. 514–520 (2021)
35. Aghababa, M.P., Haghighi, A.R., Roohi, M.: Stabilisation of unknown fractional-order chaotic systems: An adaptive switching control strategy with application to power systems. IET Gener. Transm. Distrib. 9 (14), 1883–1893 (2015)
36. Rahimi, A.M., Emadi, A.: Active damping in DC/DC power electronic converters: A novel method to overcome the problems of constant power loads. IEEE Trans. Ind. Electron. 56 (5), 1428–1439 (2009)
37. Olfati-Saber, R., Fax, J.A., Murray, R.M.: Consensus and cooperation in networked multi-agent systems. Proc. IEEE 95 (1), 215–233 (2007)

How to cite this article: Abadi, S.A.G.K., Khalili, T., Habibi, S.I., Bidram, A., Guerrero, J.M.: Adaptive control and management of multiple nano-grids in an islanded dc microgrid system. IET Gener. Transm. Distrib. 17, 1799–1815 (2023).
https://doi.org/10.1049/gtd2.12556